Polar asymmetry of $La_{(1-\delta)}Al_{(1+\delta)}O_3/SrTiO_3$ heterostructures probed by optical second harmonic generation

Andrea Rubano,[1] Gabriele De Luca,[1,a)] Jürgen Schubert,[2] Zhe Wang,[3] Shaobo Zhu,[3] Darrell G. Schlom,[3,4] Lorenzo Marrucci,[1] and Domenico Paparo[1,b)]
[1]*CNR-SPIN and Università Federico II, Monte S. Angelo, via Cintia, Napoli 80126, Italy*
[2]*Peter Grünberg Institute (PGI9-IT), JARA- Fundamentals of Future Information Technology, Research Centre Jülich, Jülich D-52425, Germany*
[3]*Department of Materials Science and Engineering, Cornell University, Ithaca, New York 14853, USA*
[4]*Kavli Institute at Cornell for Nanoscale Science, Ithaca, New York 14853, USA*

(Received 21 May 2015; accepted 1 September 2015; published online 11 September 2015)

By combining transport measurements and optical second harmonic generation, we have investigated heterostructures formed between crystalline thin films of $LaAlO_3$, with varying stoichiometry and TiO_2-terminated $SrTiO_3(001)$ substrates. Optical second harmonic generation directly probes the polarity of these heterostructures, thus complementing the transport data. The stoichiometry and the growth temperature are found to be critical parameters for controlling both the interfacial conductivity and the heterostructure polarity. In agreement with the previous work, all of the samples display an insulator-to-metal transition in the Al-reach region, with the conductivity first increasing and then saturating at the highest Al/La ratios. The second harmonic signal also increases as a function of the Al/La ratio, but, at the highest growth temperature, it does not saturate. This unusual behavior is consistent with the formation of an ordered structure of defect dipoles in the $LaAlO_3$ film caused by the off-centering of excess Al atoms in agreement with the theory. © *2015 AIP Publishing LLC*. [http://dx.doi.org/10.1063/1.4930881]

Interfacing different oxide materials together with atomic-level control has recently attracted significant attention because their physical properties can be readily tuned. Tuning material parameters allows one to design and realize novel functionalities and phenomena including charge, orbital, and spin reconstructions, magneto-electric coupling, superconductivity, and the quantum Hall effect.[1]

Among many interesting effects, the discovery of a high-mobility 2-dimensional electron gas (2DEG) at the interface between $LaAlO_3$ and $SrTiO_3(001)$ (LAO/STO), two insulating perovskites,[2] is perhaps one of the most fascinating recent examples of interface-related phenomena. The 2DEG formation is a threshold process: for $n \geq 4$ monolayers of LAO on STO, the interface becomes metallic[3] and even superconducting,[4] and the insulator-to-metal transition can be reversibly induced by an external electric field in the $n = 3$ samples.[3] It was recently demonstrated that the chemical composition (Al/La ratio) of the LAO overlayer is a critical parameter for the onset of a metallic state.[5,6] In particular, in Ref. 5, samples with nominal formula $La_{(1-\delta)}Al_{(1+\delta)}O_3$ were grown by molecular-beam epitaxy (MBE), and only Al-rich ($(1+\delta)/(1-\delta) > 1.03$) samples were found to be conductive. The experimental observations of Ref. 5 were supported by detailed first principles calculations, which determined the energetically favored defects present in $La_{(1-\delta)}Al_{(1+\delta)}O_3$ films grown on STO as a function of Al/La ratio. The excess Al in Al-rich films was found to incorporate substitutionally on the La sites of the LAO film. Importantly, due to off-centering of the Al when it substitutes for La, a dipole moment results which might break the inversion symmetry of the LAO film with a consequent enhancement of the overall polarity of the $La_{(1-\delta)}Al_{(1+\delta)}O_3$/STO heterostructure.

To investigate this point, we complemented transport data with optical second harmonic generation (SHG) measurements. In the last decade, SHG has emerged as a powerful tool for investigating polar-nonpolar oxide interfaces.[7–14] SHG denotes the generation of an optical wave with frequency 2ω by an incident wave of frequency ω. This process is determined by the constitutive relation $P_i(2\omega, z) = \varepsilon_0 \chi_{ijk}(z) E_j(\omega, z) E_k(\omega, z)$, where z is the coordinate normal to the interface, $\mathbf{P}(2\omega, z)$ is the induced second-order optical polarization, $\mathbf{E}(\omega, z)$ is the electric field of the incident wave, and $\hat{\chi}$ is the SHG susceptibility tensor. The SHG intensity I_{SHG}, as measured experimentally, is proportional to the square of the reflected SHG electric field

$$I_{SHG} \propto \left| \int_0^{d_{polar}} \mathbf{P}(2\omega) dz \right|^2, \quad (1)$$

where d_{polar} denotes the overall thickness of the SHG-active heterostructure volume.

The generation of light with double frequency, in any material, requires a breaking of the inversion symmetry.[18] Compared with the standard optical techniques, an advantage of SHG is that its probing depth is not *a priori* fixed, but depends on the spacial extent, d_{polar}, of the polar asymmetry at the specific interface and/or other regions of the heterostructure. Therefore, it only senses the heterostructure property of interest here and is insensitive to the nonpolar background.

In our past work, we have clearly demonstrated that, at the wavelength used in the following experiment, d_{polar}

a)Present address: Department of Materials, ETH Zurich, Vladimir-Prelog-Weg 4, Zurich 8093, Switzerland.
b)Electronic mail: domenico.paparo@spin.cnr.it

identifies the thickness of a very thin layer of STO close to the interface, where a quantum well is formed as a consequence of the charge confinement at the interface.[15–17] No contribution to SHG was generated from the volume of STO and LAO or from the LAO-air interface. This is because STO and LAO are centrosymmetric and their bulk volumes are SHG inactive. In contrast, we speculate below that, at specific growth temperature, an excess of Al leads to the formation of a structure of ordered defect dipoles that breaks the inversion symmetry of the LAO film, thus leading to an enhancement of the SHG generated from the $La_{(1-\delta)}Al_{(1+\delta)}O_3$/STO heterostructure.

The SHG experimental layout is given in Fig. 1(a). The light source is an amplified pulsed laser (pulse duration—35 fs, repetition rate—1 KHz, pulse energy—4 mJ, central wavelength—800 nm). At this wavelength, the SHG signal is off of any electronic resonance of the interface,[12] allowing a direct coupling of the SHG yield to the heterostructure polarity without the complication of the optical selection rules acting at the resonances.[11] The pulses are adjusted in energy and in polarization by appropriate optical components and focused onto the sample surface by a lens with a 300 mm of focal length, resulting in a beam diameter of $300 \pm 14\ \mu$m on the sample surface. The SHG signal is spectrally separated from the reflected fundamental by colored filters and a monochromator and finally measured by a photon multiplier. Both the input fundamental and the output SHG beams are linearly polarized. In what follows, the labels *p*, *s*, and *d* denote linear polarizations, respectively, parallel, perpendicular, or at 45° with respect to the plane of incidence of light. In accordance with the four-fold rotational symmetry (4 mm) of the interface, we measured the all three independent non-vanishing SHG components: *p*-in *p*-out (*pp*), *s*-in *p*-out (*sp*), and *d*-in *s*-out (*ds*).[11] These three measurements entirely quantify the SHG yield of these interfaces. We note that this assumption holds true for the ultrathin LAO film too for which, being the light wavelength much larger of its thickness, we can neglect the width along the perpendicular to the surface and consider it as an interfacial layer. The samples were placed in the same position with respect to the beam focus with about 100 μm accuracy, in order to ensure that any change in the observed SHG yield could not be ascribed to a change in the laser fluence due to a different spot-size on the sample surface. Measurements have been performed at room temperature several times, on different days, and sample order, and all the reported experimental error-bars refer to fluctuations over repeated measurements (confidence level of 66%, one σ). Samples having eight LAO monolayers were grown simultaneously on a line of substrates mounted on a sample holder (Fig. 1(b)), with a monotonic variation in the Al/La ratio of the LAO according to the relative position of the substrate with respect to the sources in the MBE system. With lanthanum and aluminum fluxes calibrated to within a few percent, the gradient in the Al/La ratio ensured that at some position on the line, quasi-stoichiometric LAO was deposited. For all other points on the line, a non-stoichiometric layer composition with formula $La_{(1-\delta)}Al_{(1+\delta)}O_3$ is obtained. In order to estimate the exact value of δ in different samples, a companion calibration sample-set was grown on which *ex situ* Rutherford Backscattering Spectroscopy (RBS) measurements were performed to determine the chemical composition (see supplementary material in Ref. 5 for details). The value of δ for the actual set of 9 samples (labeled a, b,…, i) is finally extracted by linear interpolation, and the results for the Al/La ratio are displayed in lower line of Fig. 1(b).

Three sets of samples have been grown at different substrate temperatures, namely, at 720 °C, 755 °C, and 790 °C, measured by means of an optical pyrometer. Figure 2 shows the sheet conductance as a function of the Al/La ratio: in

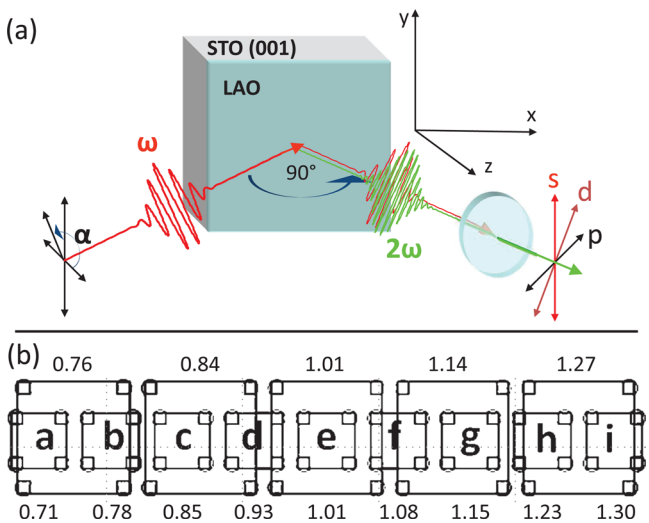

FIG. 1. Panel (a) shows a schematic layout of the experiment: light with fundamental frequency ω hits the sample surface with adjustable polarization angle, $\alpha = s, p, d$, where *s* is the direction parallel to the sample surface, *p* is parallel to the incidence plane, and *d* is at 45° between the two. The second harmonic light at frequency 2ω is then filtered to remove the reflected fundamental and analyzed. Panel (b) shows the relative position in the growth chamber of the $5 \times 5\ mm^2$ samples used for the experiment (labeled by letters a, b, …, i) and the $10 \times 10\ mm^2$ companion samples used for RBS experiments to calibrate the Al/La ratio. The experimental values of this ratio and the values computed by linear interpolation are displayed above and below the image, respectively.

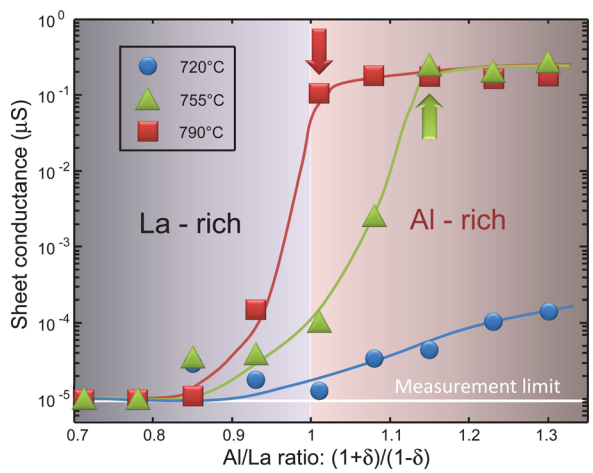

FIG. 2. Sheet conductance as a function of the Al/La ratio. Different colors refer to samples grown at different temperatures: 720 °C (blue circles), 755 °C (green triangles), and 790 °C (red squares). The shadowed areas denote the two non-stoichiometric chemical compositions, La-rich and Al-rich, respectively. The shadow gradient indicates the direction of increasing chemical component in the respective areas. The horizontal white line denotes the measurement limit. The red and green arrows indicate the insulator-to-metal transition points for the samples grown at 790 and 755 °C, respectively. Solid lines are a guide for the eyes.

agreement with the previous results, only the Al-rich samples are conductive.[5] As the Al amount is increased, the conductivity clearly saturates. In addition, the sample conductivity is very low for the sample-set grown at the lowest temperature (720 °C), while it is about 3 orders of magnitude higher in the case of 790 °C. For the sample-set grown at 755 °C, the conductivity appears for larger values of the Al content compared with the 790 °C set. The two arrows in Fig. 2 indicate the conductive samples with the lowest Al-content for the 790 °C set (red arrow) and the 755 °C set (green arrow), respectively. In Fig. 3, the SHG intensity measured for all the samples indicated in Fig. 1 and labeled with letters (a–i) is reported for all the three sets of temperatures: 720 °C (blue circles), 755 °C (green triangles), and 790 °C (red squares). The three panels show the SHG intensity for the three polarization combinations: (a) *pp*, (b) *ds*, and (c) *sp*. For comparison, the SHG intensity measured from the surface of a pure, TiO_2-terminated STO substrate is included (orange stars).

Starting from the data shown in Fig. 3, the total SHG yield, $\bar{I}_{SHG}$, may be calculated. $\bar{I}_{SHG}$ is shown as a function of the Al/La ratio and for all the growth temperatures in Fig. 4. These values have been normalized to that found for the STO-air interface. Incidentally, we observe that the square root of these values provides with an estimate of the quantum well depth formed at the LAO/STO interface when the SHG signal may be attributed to this source alone.[13] This is presumably true for all the samples grown at the lowest substrate temperatures and for the La-enriched samples grown at the highest temperature.

$\bar{I}_{SHG}$ of the samples grown at 720 °C is only slightly increasing in the Al-rich region of the diagram, while it strongly increases for the other two sets. In particular, the

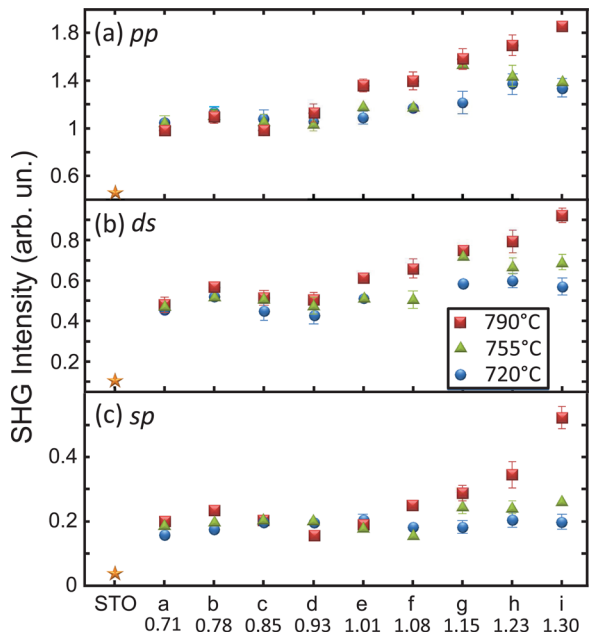

FIG. 3. SHG intensity as measured for all the samples indicated in Fig. 1 and labeled with letters (a–i) for all the substrate temperatures: 720 °C (blue circles), 755 °C (green triangles), and 790 °C (red squares). Below the letters (a–i), the corresponding Al/La ratios are indicated too. The three panels show the SHG intensity for the three polarization combinations: (a) *pp*, (b) *ds*, and (c) *sp*. For comparison, the SHG intensity measured from a pure STO substrate is included (orange stars).

790 °C-set sample with the highest content of Al displays a total SHG yield that is about twice that of the quasi-stoichiometric samples in the same set. The same sample shows an increase of $\bar{I}_{SHG}$ of about 50% compared with that of the 755 °C set with the same Al/La ratio. The latter result is particularly striking if we consider that the conductivity for these samples is approximately the same or even slightly higher for the set grown at 755 °C. It is also interesting to note that, while the conductivity of the 790 °C-set samples saturates by increasing the Al content, $\bar{I}_{SHG}$ does not show the same behavior. Conversely, the 755 °C sample set shows a saturation behavior similar to the corresponding conductivity. Additionally, we note that the points where the values of $\bar{I}_{SHG}$ for the 755 °C and 790 °C sets start to increase are perfectly matching the onset of conduction as highlighted by the red and green arrows.

The observed effect of film growth temperature on the observed SHG signal and film conductivity appears unusual. Nonetheless, we present a speculative explanation below that is qualitatively consistent with the expectations from theory.[5] The first principles calculations performed by Warusawithana *et al*. determined the energetically favored defects present in $La_{(1-\delta)}Al_{(1+\delta)}O_3$ films grown on STO as a function of Al/La ratio.[5] The excess Al in Al-rich films was found to incorporate substitutionally on the La sites of the LAO crystal. In La-rich films, however, the excess La was found to not substitute on the Al sites of the LAO crystal because it is too large; instead Al_2O_3-vacancy complexes form in La-rich films. These different defect structures (few cation vacancies in Al-rich films vs. many cation vacancies in La-rich films) result in a significantly higher diffusion coefficient for cations in the La-rich films. This higher diffusion coefficient makes it possible for the diverging electric potential caused by the atomic layer arrangement at the interface between $La_{(1-\delta)}Al_{(1+\delta)}O_3$ and TiO_2-terminated STO to be accommodated by Al vacancies in La-rich films.[5] This is why no interfacial conductivity is observed in the La-rich films. In the Al-rich films, the low diffusion coefficient of cations results in the diverging electric potential to be compensated by electronic reconstruction, which gives rise to interfacial conductivity in the Al-rich films. The dependence of the conductivity on growth temperature may result from the combination of local fluctuations in the Al/La ratio in the $La_{(1-\delta)}Al_{(1+\delta)}O_3$ films with the need for a percolative network of conducting regions before conductivity is seen in the transport measurements. At low growth temperature, the local composition fluctuations are largest. This shifts the Al/La ratio needed to produce a percolative conduction network to higher Al/La ratio. This speculative explanation is consistent with the observed saturation in the sheet conductance that occurs in the Al-rich films grown at 755 °C and 790 °C; it saturates when the Al-excess swamps out local composition variations and the entire 2DEG is connected via percolation.

As already stated, the substitution of La by Al in Al-rich samples is accompanied by the formation of defect dipoles due to off-centering of substitutional Al-atoms.[5] These dipole moments can be oriented by the initial electric field building in LAO before the electronic reconstruction occurs. This gives rise to a structure of ordered defect dipoles that breaks the LAO inversion symmetry. This leads to an

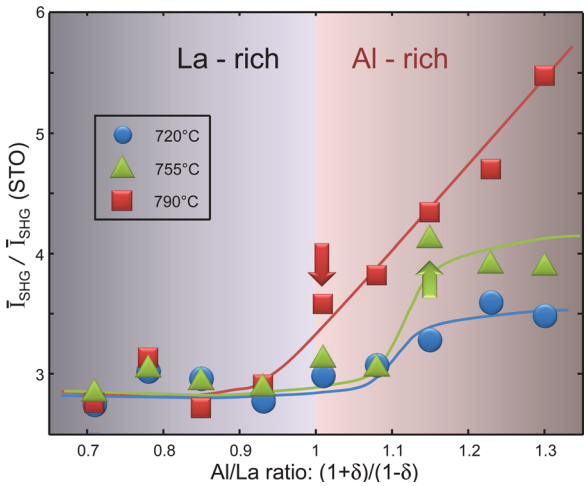

FIG. 4. The total SHG yield as a function of the Al/La ratio, normalized to the value found for the STO-air interface. The two arrows indicate the onset of conduction for the 790 °C-set (red) and the 755 °C-set (green) samples. The shadowed areas denote the two non-stoichiometric chemical compositions, La-rich and Al-rich, respectively. The shadow gradient shows the increase direction of the chemical component in each respective area. Solid lines are a guide for the eyes.

additional SHG signal that adds to the one caused by the formation of the quantum well at the LAO/STO interface alone. Conversely to conductivity, at the highest substrate temperature, this SHG signal does not saturate or saturates at very high Al-excess, since an increase of Al atoms is directly accompanied by the formation of new SHG-active defect dipoles. The same behavior is not observed at the lowest substrate temperatures, possibly due the capacity of excess Al to hamper crystallization in the $La_{(1-\delta)}Al_{(1+\delta)}O_3$ film. Under Al-rich growth conditions as the growth temperature is lowered, an increasing volume of the $La_{(1-\delta)}Al_{(1+\delta)}O_3$ film is amorphous and Al excess in this amorphous matrix results in no defect dipoles. On the other hand, an increase of the substrate temperature opposes this glass-forming tendency. A substrate temperature of 790 °C is sufficient to keep the $La_{(1-\delta)}Al_{(1+\delta)}O_3$ film crystalline everywhere so that Al substituting onto the La sites may produce defect dipoles. This explains the anomalous behavior of SHG as a function of the Al/La ratios for the sample set grown at the highest temperature.

In summary, we have investigated the mutual influence of the LAO stoichiometry and growth temperature on the conductivity and polarity of $La_{(1-\delta)}Al_{(1+\delta)}O_3$/STO heterostructures. We have found that the conductivity and the polarity of the heterostructures grown at the highest substrate temperatures behave differently as a function of the Al/La ratio. In particular, while conductivity saturates, the polarity of the $La_{(1-\delta)}Al_{(1+\delta)}O_3$ film increases without saturating. We propose that this unusual behavior is a consequence of the formation of an ordered structure of defect dipoles in the $La_{(1-\delta)}Al_{(1+\delta)}O_3$ film due to the off-centering of excess Al-atoms. This ordered structure may be formed only at sufficiently high substrate temperatures, since such conditions are necessary to counteract the tendency of an Al-excess to hamper the crystallization of the $La_{(1-\delta)}Al_{(1+\delta)}O_3$ film.

We acknowledge funding from the European Union (FP7-PEOPLE-2012-CIG, Grant Agreement No. PCIG12-GA-2012-326499-FOXIDUET), from the Ministero dell'Istruzione, dell'Università e della Ricerca (Grant No. PRIN 2010-11-OXIDE), and Regione Campania (L.R. 5 2002). The work at Cornell was supported by the AFOSR under Grant No. FA9550-10-1-0524.

[1]H. Y. Hwang, Y. Iwasa, M. Kawasaki, B. Keimer, N. Nagaosa, and Y. Tokura, Nat. Mater. **11**, 103 (2012).
[2]A. Ohtomo and H. Y. Hwang, Nature **427**, 423 (2004).
[3]S. Thiel, G. Hammerl, A. Schmehl, C. W. Schneider, and J. Mannhart, Science **313**, 1942 (2006).
[4]N. Reyren, S. Thiel, A. D. Caviglia, L. F. Kourkoutis, G. Hammerl, C. Richter, C. W. Schneider, T. Kopp, A.-S. Rütschi, D. Jaccard, M. Gabay, D. A. Muller, J.-M. Triscone, and J. Mannhart, Science **317**, 1196 (2007).
[5]M. P. Warusawithana, C. Richter, J. A. Mundy, P. Roy, J. Ludwig, S. Paetel, T. Heeg, A. A. Pawlicki, L. F. Kourkoutis, M. Zheng, M. Lee, B. Mulcahy, W. Zander, Y. Zhu, J. Schubert, J. N. Eckstein, D. A. Muller, C. S. Hellberg, J. Mannhart, and D. G. Schlom, Nat. Commun. **4**, 2351 (2013).
[6]E. Breckenfeld, N. Bronn, J. Karthik, A. R. Damodaran, S. Lee, N. Mason, and L. W. Martin, Phys. Rev. Lett. **110**, 196804 (2013).
[7]A. Savoia, D. Paparo, P. Perna, Z. Ristic, M. Salluzzo, F. Miletto Granozio, U. Scotti di Uccio, C. Richter, S. Thiel, J. Mannhart, and L. Marrucci, Phys. Rev. B **80**, 075110 (2009).
[8]A. Rubano, M. Fiebig, D. Paparo, A. Marino, D. Maccariello, U. Scotti di Uccio, F. Miletto Granozio, L. Marrucci, C. Richter, S. Paetel, and J. Mannhart, Phys. Rev. B **83**, 155405 (2011).
[9]T. Günter, A. Rubano, D. Paparo, M. Lilienblum, L. Marrucci, F. Miletto Granozio, U. Scotti di Uccio, R. Jany, C. Richter, J. Mannhart, and M. Fiebig, Phys. Rev. B **86**, 235418 (2012).
[10]A. Rubano, T. Günter, T. Fink, D. Paparo, L. Marrucci, C. Cancellieri, S. Gariglio, J.-M. Triscone, and M. Fiebig, Phys. Rev. B **88**, 035405 (2013).
[11]D. Paparo, A. Rubano, and L. Marrucci, J. Opt. Soc. Am. B **30**, 2452–2460 (2013).
[12]A. Rubano, C. Aruta, U. S. di Uccio, F. M. Granozio, L. Marrucci, T. Günter, T. Fink, M. Fiebig, and D. Paparo, Phys. Rev. B **88**, 245434 (2013).
[13]G. De Luca, A. Rubano, E. di Gennaro, A. Khare, F. M. Granozio, U. S. di Uccio, L. Marrucci, and D. Paparo, Appl. Phys. Lett. **104**, 261603 (2014).
[14]A. Rubano, T. Günter, M. Lilienblum, C. Aruta, U. S. di Uccio, F. M. Granozio, L. Marrucci, D. Paparo, and M. Fiebig, Appl. Surf. Sci. **327**, 413 (2015).
[15]Z. S. Popovic and S. Satpathy, Phys. Rev. Lett. **94**, 176805 (2005).
[16]K. Yoshimatsu, R. Yasuhara, H. Kumigashira, and M. Oshima, Phys. Rev. Lett. **101**, 026802 (2008).
[17]L. X. Hayden, R. Raimondi, M. E. Flatte, and G. Vignale, Phys. Rev. B **88**, 075405 (2013).
[18]Y. R. Shen, Surf. Sci. **299/300**, 551 (1994).